Structural Transition of Bacteriorhodopsin Is Preceded by Deprotonation of Schiff Base: Microsecond Time-Resolved X-Ray Diffraction Study of Purple Membrane

Toshihiko Oka,*† Katsuaki Inoue,† Mikio Kataoka,‡ and Naoto Yagi†

*Department of Physics, Faculty of Science and Technology, Keio University, Kohoku, Yokohama, Kanagawa, Japan; †Life and Environmental Science Division, Japan Synchrotron Radiation Research Institute, Mikazuki, Sayo, Hyogo, Japan; and ‡Graduate School of Material Science, Nara Institute of Science and Technology, Ikoma, Nara, Japan

ABSTRACT The structural changes in the photoreaction cycle of bacteriorhodopsin, a light-driven proton pump, was investigated at a resolution of 7 Å by a time-resolved x-ray diffraction experiment utilizing synchrotron x rays from an undulator of SPring-8. The x-ray diffraction measurement system, used in coupling with a pulsed YAG laser, enabled us to record a diffraction pattern from purple membrane film at a time-resolution of 6 μs over the time domain of 5 μs to 500 ms. In the time domain, the functionally most important M-intermediate appears. A series of time-resolved x-ray diffraction data after photo-excitation showed clear intensity changes caused by the conformational changes of helix G in the M-intermediate. The population of the reaction intermediate was prominently observed at ~5 ms after a photo-stimulus. In contrast, absorption measurement indicated the deprotonation of the Schiff base predominantly occurred at ~300 μs after a photo-stimulus. These results showed that the conformational changes characterizing structurally the M-intermediate predominantly occur at a later stage of the deprotonation of the Schiff base. Thus, the M-intermediate can be divided into two metastable stages with different physical characteristics.

INTRODUCTION

Bacteriorhodopsin (BR) produced on the cell membrane of *Halobacterium sallinarium* is a light-driven proton pump, transporting a proton unidirectionally from the cytoplasm to the extracellular medium by utilizing photon energy. BR is composed of a bacterioopsin (248 residues) and a retinal, serving as a chromophore connected to the apoprotein via a Schiff base with a lysine residue (Haupts et al., 1999). The structure of BR comprises seven transmembrane helices (A–G), and the trimer of BR molecules is organized into a two-dimensional crystalline array, named purple membrane (PM). Upon absorbing light, the photo-isomerization of all-trans retinal to 13-*cis* configuration triggers the characteristic photoreaction cycle going through metastable photointermediates (J, K, L, M, N, and O) characterized by their absorption spectra.

In the photoreaction cycle, the most important intermediate for unidirectional proton pumping is the M, where the deprotonation of the Schiff base occurs. Kinetic studies on the absorption changes in the photocycle suggest the existence of two types of M-intermediate, named M_1 and M_2 with different kinetic constants (Váró and Lanyi, 1991a,b). The transition from M_1 to M_2 occurs irreversibly. Thus, it has been proposed that the Schiff base switches the access from the extracellular side to the cytoplasmic side during the M_1–M_2 transition. Other spectroscopic studies also pointed out the existence of two types of M-intermediate (Druckmann et al., 1992; Rödig and Siebert, 1999) and the coupling the transition with the proton release into the extracellular medium (Zimanyi et al., 1992).

Several crystal structure analyses of the M-intermediate have been reported for wild-type and mutant BRs. The reported structures seem to be classified into two groups with respect to the magnitude of conformational changes from the ground state. In some crystal structures, the conformational changes are limited to local residues surrounding the Schiff base (Facciotti et al., 2001; Lanyi and Schobert, 2002, 2003). In contrast, the other structures displayed large conformational changes in the cytoplasmic halves of helices F and G (Luecke et al., 1999; Sass et al., 2000). Thus, M-intermediates with the small and the large conformational changes are designated as ''early M'' and ''late M'', respectively.

The spectroscopically observed M_1 and M_2 intermediates may correspond to the structurally identified ''early'' and ''late'' M-intermediates. It was, however, difficult to distinguish whether or not the ''late'' M-intermediate actually appeared after the ''early'' M-intermediate, since crystallographic studies carried out at low temperature provide little information about the time course of structural changes. In addition, BR molecules in crystal are under the influences of crystal contacts, which restrict structural changes around contact surfaces. Thus, there are a couple of questions we need to answer: 1), What is the substantial difference between the two meta-stable M-intermediates? 2), Does the protonation of the Schiff base and structural changes in the helices occur simultaneously, or not?

Submitted August 24, 2004, and accepted for publication October 13, 2004.

Address reprint requests to Toshihiko Oka, Dept. of Physics, Faculty of Science and Technology, Keio University, 3-14-1 Hiyoshi, Kohoku, Yokohama, Kanagawa 223-8522 Japan. Fax: 81-45-566-1672; E-mail: oka@phys.keio.ac.jp.

0006-3495/05/01/436/07 $2.00

doi: 10.1529/biophysj.104.051748

To answer the questions, time-resolved x-ray diffraction technique is one of the suitable methods to trace structural changes. The technique is advantageous to keep the physiological conditions of the sample. In the previous study, we measured the M–N structural transitions with the technique applied for PM (Oka et al., 2000). It was, however, impossible to apply the previous measurement system to clarify the two questions, because the hypothetical intermediate was expected to appear in the time domain of microseconds to milliseconds. Thus, we developed a new measurement system for time-resolved diffraction at the beamline BL40XU of the synchrotron facility SPring-8, and the system enabled us to carry out time-resolved diffraction experiments at a time-resolution of 6 μs (Oka et al., 2004). The time-resolved x-ray diffraction patterns of PM displayed significant changes in intensities particularly in the milliseconds region. The data analyzed by the singular value decomposition (SVD) method demonstrated that the structural change of the G-helix is preceded by the deprotonation of the Schiff base. This result probably contributes to the understanding of the molecular mechanism underlying the proton pumping by BR.

MATERIALS AND METHODS

Sample preparation

PM of wild-type BR was isolated from *H. salinarium* according to a conventional method (Oesterhelt and Stoeckenius, 1974). Isolated PM was concentrated in a buffer containing 10 mM MOPS (pH 7.0) so that the absorbance of the solution was 20. The sample for spectroscopic and diffraction measurements was prepared by the following procedure. A layer of PM was made by drying a 15 μl-drop of the suspension on a polyethylene film of 10-μm thickness or quartz plate of 20-μm thickness. This procedure was iterated two times on the dried layer. The resultant sample, whose absorbance at 568 nm was ~3, was sealed in a sample cell at 298 K for absorption and x-ray diffraction measurements. The relative humidity was kept at 75% by setting a drop of saturated NaCl solution (O'Brien, 1948) in the sealed sample cell.

Time-resolved absorption measurements

Flash-induced absorption changes of PM were monitored at 410 nm by using a flash-photolysis measurement system (UNISOKU, Osaka, Japan). The increase of the absorption at 410 nm reflects the deprotonation of the Schiff base in BR. The time range measured was from 0.4 μs to 150 ms by varying the time-resolution from 0.4 μs to 20 μs, and data were taken 32 times at intervals of 10 s between photo-triggers with flashlight from a frequency-doubled Nd-YAG laser (Surelite-I, Continuum, Santa Clara, CA). The sample was illuminated from one side with an irradiance of ~50 μJ/mm^2 reduced by ND filters (Sigma Koki, Tokyo, Japan).

Time-resolved x-ray diffraction experiments

Time-resolved x-ray diffraction experiments were carried out at the beamline BL40XU of SPring-8 (Inoue et al., 2001) by using a system for time-resolved measurements enabling a time-resolution of 6 μs (Oka et al., 2004). The undulator source was tuned to emit x-rays with an energy peak at 15.0 KeV and width of 1.8% (Inoue et al., 2001). PM samples were kept at 298 K and 75% relative humidity as well as the spectroscopic measurements. The plane of the sample was set to be normal to incident x-ray beam. To initiate photocycle of BR efficiently, the sample was obliquely illuminated from both sides by laser pulses of the frequency-doubled Nd-YAG laser Surelite-II-10 (Continuum). ND filters (Sigma Koki) were placed in the laser path to reduce the irradiance of laser pulse to ~50 μJ/mm^2. Diffraction patterns up to a resolution of 7 Å were recorded with a C4880-50-24A CCD camera (Hamamatsu Photonics, Hamamatsu, Japan) coupled with a 6-inch x-ray image intensifier V5445P (Hamamatsu Photonics) (Fujisawa et al., 1999) placed at 420 mm from the sample. A vacuum path was set between the sample and the detector to reduce absorption and scattering caused by air.

The sequence of the time-resolved measurement was as follows: The sample was irradiated by a laser pulse of 5 ns and then exposed to an x-ray pulse of 6 μs width. The delay-time between the laser and x-ray pulses was varied from 5 μs to 500 ms (see Results). The interval of photo-triggers was adjusted to 1 s. To reduce read-out noise of the CCD camera system, the exposure time was limited to 20 s, thus, 19 diffraction patterns with the same delay-time were accumulated in one CCD image. The position x-rays exposed was slid before damage in diffraction pattern or bleach of the sample became obvious. Estimated dose of x-rays at same position was $\sim 7 \times 10^3$ Grays.

Data analysis by the SVD and difference Fourier methods

A circular averaging procedure was applied to a set of the time-resolved powder diffraction patterns. To ensure the good statistics, 152 data sets were averaged for the same delay-time.

A set of the profiles was equivalent to a matrix $A(S,t)$, the matrix element A_{ij} of which corresponds to the intensity at the ith scattering vector S_i and jth delay-time t_j. Such an $m \times n$ matrix was decomposed with the SVD method (Henry and Hofrichter, 1992; Oka et al., 2000) as

$$A(S, t) = U(S)S_V V(t)^T,$$

where $U(S)$, S_V and (t) are a $m \times n$, a $n \times n$ diagonal, and a $n \times n$ matrices. The elements of matrix $U(S)$ described the orthonormal basis spectra of $A(S,t)$. The values of the diagonal component in matrix S_V, called singular value, indicated the contribution of the basis spectra to $A(S,t)$. The component of $V(t)$ described the time-dependent variation of the basis spectra.

The spectral dispersion of incident x-rays (Inoue et al., 2001) was deconvoluted from the $U(S)$ spectra. Then, the integrated intensities of Bragg reflections were calculated using the least-square fitting method with Gauss functions. For Fourier map calculation, the ratio separating the overlapping asymmetric reflections from the powder pattern and the phase values of all reflections were taken from the results of a cryoelectron microscopy study for PM (Henderson et al., 1990). Most of the calculations were carried out with Igor Pro4 (Wavemetrics, Lake Oswego, OR).

RESULTS

Time-resolved absorption measurement

The absorption change at 410 nm reflects the amount of M-intermediate with deprotonated Schiff base, because the other photointermediates with protonated Schiff base show negligible absorption changes and extinction coefficients at 410 nm. Under these conditions, N and O intermediates accumulate in very little amounts in PM samples (Váró and Lanyi, 1991b). Fig. 1 shows the absorption change at 410 nm after a flash excitation of PM film. Only 12% of BR molecules is initiated its photocycle with the flash. The time-dependent variation displays a broad maximum at ~300 μs

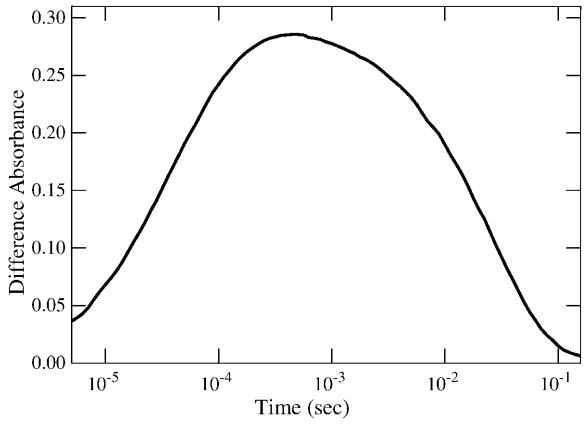

FIGURE 1 Time course of difference absorbance at 410 nm of PM film. Photoreaction was started with a flash pulse from YAG-laser (532 nm). The absorbance of the sample was almost the same with that for x-ray diffraction experiments.

and a shoulder at ~5 ms, indicating that the deprotonation of BR molecule within the M-intermediate is likely to go through at least two conformational substates rather than only one single state. The absorption changes at 410 nm reversibly occur under iterative photo-stimuli at least for 4 h.

X-ray diffraction profiles in the time-resolved measurement

Fig. 2 *a* displays the time-resolved x-ray diffraction profiles from 5 μs to 500 ms, and Fig. 2 *b* demonstrates the difference profiles subtracted an averaged profile before photo-trigger. The profile changes are small as expected from the time-resolved absorption measurement shown in Fig. 1, however, intensity changes are significant enough to trace the time course of structural change. Diffraction intensities increase gradually until 5 ms after photo-trigger and return to a noise-level after 100 ms (Fig. 2 *b*). The profiles before photo-trigger are almost the same during the iterative accumulation of diffraction data, and the intensity changes reversibly appeared. These results indicate that little radiation damages occur under these experimental conditions and that the intensity changes must come from the structural changes of BR.

In the difference profile at ~5 ms (Fig. 2 *b*), the magnitudes of the positive peak at (11) reflection and the negative at (20) are comparable. As reported previously (Kamikubo et al., 1997), the magnitude ratio of intensity difference between (11) positive and (20) negative peaks is 1:1 in the difference profile in the M-intermediate, whereas that is 1:0 in the N-intermediate. Thus, the M-intermediate is the major component in the sample. Intensity changes in (11) and (20) reflections at ~5 ms are about one-fifth of those observed in PM sample fully accumulating the M-intermediate (Nakasako et al., 1991). Thus, the efficiency for photo-excitation of BR by this system under these conditions

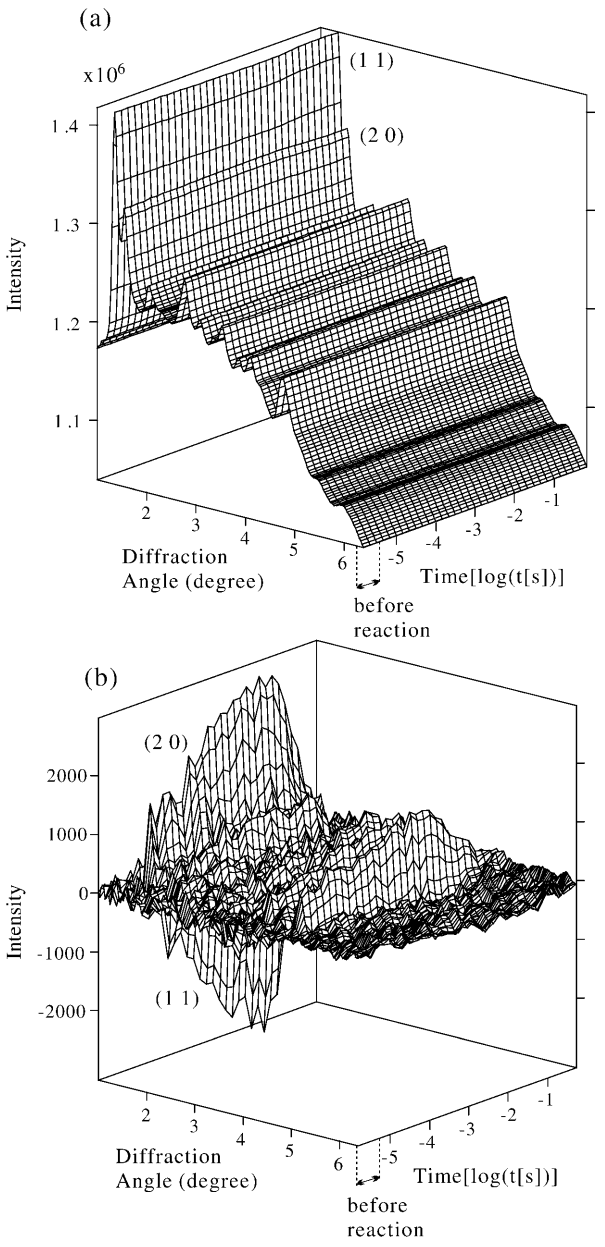

FIGURE 2 (*a*) Time-resolved x-ray diffraction profiles of PM films. First four frames are taken before photoreaction. (*b*) Difference diffraction profiles calculated by subtracting the averaged profile before the photoreaction from each frame.

is ~20%. This value is about twice that observed in the absorption measurement, where the laser pulse exciting BR molecules irradiated only one side of the sample.

SVD analysis of the time-resolved diffraction data

In the SVD analysis applied for the time-resolved data, only two components have significant singular values in the S_V matrix and are sufficient to reproduce the data (Fig. 3). The

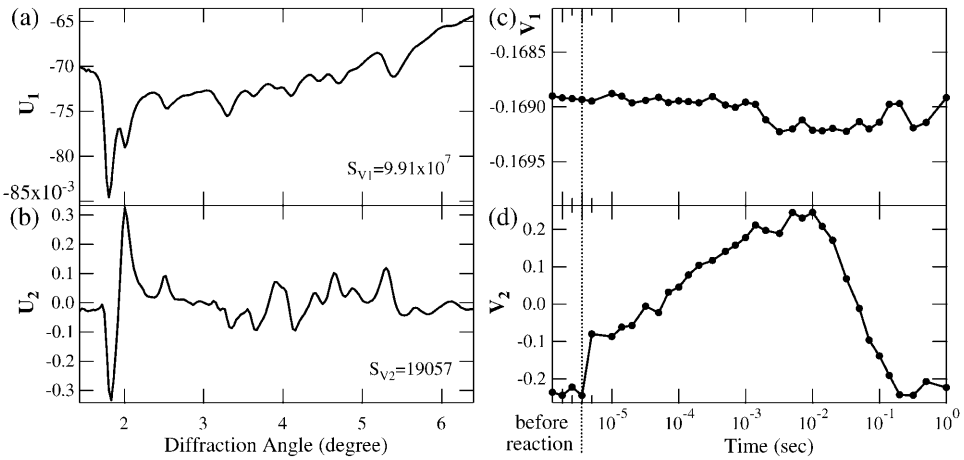

FIGURE 3 (*a* and *b*) *U* spectra of SVD analysis for the x-ray diffraction data in Fig. 2 *a*. These panels show two major components, U_1 and U_2, with their singular values. (*c* and *d*) *V* spectra of SVD analysis. These spectra indicate the time-dependent variations of corresponding *U* spectra.

third component conjugates with a small singular value and contains noise even in the region of diffraction peaks (data not shown). Thus, the components higher than the third are negligible from the following analyses.

Fig. 3 *a* shows the first component of the *U* matrix, U_1, which is similar to the diffraction pattern before photoexcitation except for its negative sign. The negative sign of the component compensates the negative sign of the first component of the *V* matrix, V_1. Because V_1 shows no time-dependence even at the laser excitation, U_1 mostly describe the diffraction pattern before photoreaction.

The second component U_2 (Fig. 3 *b*) has a profile very similar to the difference diffraction profile between the M-intermediate and the original state measured for PM (Nakasako et al., 1991). The second *V*-matrix component V_2, describing the time-dependent variation of U_2, shows a significant change after the flash excitation up to 5 ms and decays back to the level before photo-trigger (Fig. 3 *d*). The time course is nearly parallel to that observed in the raw data in Fig. 2.

Two components identified in the SVD analysis come from two structural states in the photocycle: one intermediate state with large structural changes and another base state whose structure is almost the same with that before photoreaction. Difference profile between the intermediate and the base states must have time-dependence. Because V_1 shows very little time-dependent variation even at the laser excitation, U_1 doesn't have information about the difference. Thus, only U_2 includes the difference diffraction profiles between the intermediate and the base states, and only V_2 includes the time-dependence of the difference.

The time-dependent changes of V_2 (Fig. 3 *d*) and the absorption change at 410 nm (Fig. 1) are roughly similar, however, maximum changes appear in different timescale. Although the absorption at 410 nm maximally increases at $\sim$300 μs, intensity changes are most prominent at $\sim$5 ms after the photoreaction. It should be noted that an additional enhancement seen in at $\sim$5 ms in the absorption change may correlate with the peak in V_2.

Structural change during photocycle expected from the difference Fourier analysis

To visualize the structural changes during photocycle, we calculate a Fourier map of the U_2 component projected on the membrane plane at a resolution of 7 Å (Fig. 4). The map corresponds to the difference map between the intermediate and the base state. In the Fourier map, a pair of large positive and negative peaks appears around the G-helix. The pair is very similar to that typically observed in the projection maps of the M-intermediate (Nakasako et al., 1991; Oka et al., 2000), but not in the N or MN structure, where the structural changes are prominent around the F-helix (Kamikubo et al., 1996, 1997; Oka et al., 2000). In addition, spectroscopic study showed that the N-intermediate accumulated a negligible amount at 75% relative humidity (Váró and Lanyi, 1991b). Thus, the U_2 component must arise from the global structural changes in the M-intermediate, and the V_2 component basically displays the time-dependent population of the intermediate in the sample after photo-trigger.

As mentioned above, the time-dependent variation of diffraction change is a prominent at $\sim$5 ms. It is significantly delayed from the period of the maximum absorption change at 410 nm. Thus, it is clear that the deprotonation of the Schiff base precedes the structural change around the G-helix. In other words, the photochemically assigned M-intermediate is likely separated into two successive states regarding the structural properties. In the first state, the deprotonation of the Schiff base occurs at $\sim$300 μs accompanying local and small conformational changes. This state is assignable as early M (M_1) state. The second state is the late M (M_2) appearing at $\sim$5 ms with significant conformational changes around the G-helix detectable in x-ray diffraction pattern.

DISCUSSION

This study focuses on the global structural changes of BR in the time domain of microseconds to milliseconds during

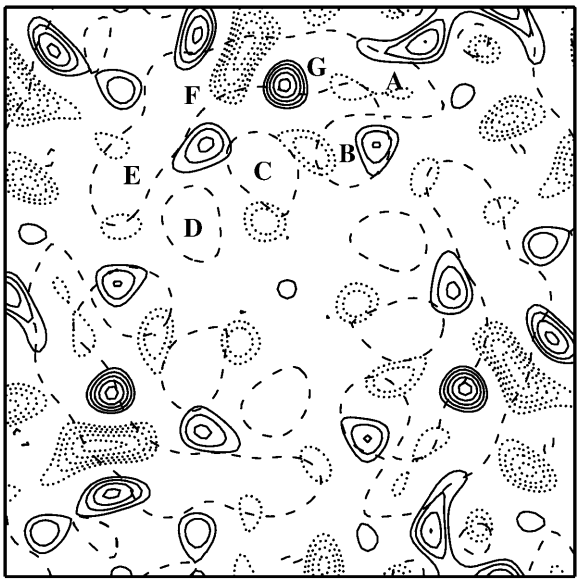

FIGURE 4 A Fourier map calculated from U_2 profile. The Fourier map corresponds to a difference Fourier map between the late M (M_2) and the original BR state before photoreaction. Solid lines indicate area with increase in electron density in the late M, and dotted lines show area with decrease. Dashed lines show outline of the BR trimer. A prominent positive peak is observed on the G-helix, and an adjacent negative peak is located between the G- and F-helices.

the photocycle. The data demonstrate clearly that the global structural change around the G-helix occurs after the deprotonation of the Schiff base.

Time-resolved x-ray diffraction experiment

The global conformational changes in BR photocycle have been hypothesized to occur in the microsecond to millisecond time domain. Though we had measured the M–N structural transition of wild-type BR and the M–MN transition of D96N mutated BR by time-resolved experiments previously (Oka et al., 2000, 2002), the time-resolution in those experiments were limited to ~100 ms because of insufficient flux of x-rays and the readout speed of the used detector system. To overcome these, a new x-ray diffraction system to trace the fast process in microsecond time domain was developed by utilizing x rays from a helical undulator (Hara et al., 2001) and a fast shutter system (Oka et al., 2004). Because of a high flux x rays of 1.0×10^{15} photons s^{-1} at 12.4 KeV at BL40XU in SPring-8 (Inoue et al., 2001), an x-ray pulse as short as 6 μs period is feasible for measuring diffraction or scattering patterns from transient state of materials (Oka et al., 2004).

Two metastable states in the M-intermediate

From the enthalpy and entropy changes, the M_1–M_2 transition is expected to associate with major conformational changes (Váró and Lanyi, 1991c). The Schiff base transfers a proton to D85 at the L–M transition and receives a proton from D96 at the M–N transition. This is explained by the idea of a switch of access: the Schiff base changes the access from extracellular to cytoplasmic side during the M-intermediate (Lanyi and Schobert, 2004). The conformational change in the G helix during the M-intermediate seems to correlate with the switch.

Static diffraction experiments for PM of D96N-BR indicated two substates of the M-intermediate: one with undetectable conformational changes and another with large changes (Sass et al., 1997; Weik et al., 1998). In addition, the structural model of the M-intermediate from cryogenic crystallography can be classified into two groups with small changes (Facciotti et al., 2001; Lanyi and Schobert, 2002, 2003) and with global structural changes (Luecke et al., 1999; Sass et al., 2000). This experimental result likely explains these observations: the experiments revealing the small structural changes of BR trapped and observed the early stage of the M-intermediate, and the large conformational changes reflect the late stage of the M-intermediate after the M_1–M_2 transition. In this regard, an interesting structure of M-intermediate was reported through a cryo-crystallography for mutated BR. In the crystal structure, the G-helix does not shift considerably, despite the retinylidene nitrogen atom of the Schiff base points toward the cytoplasmic side (Luecke et al., 2000). The state may correspond to a transient intermediate state between the M_1 and M_2. The global structural transition would take a longer time than the conformational switch in the local area. Thus, the precedence of the conformational switch at the Schiff base is most likely if the switch of the Schiff base induces the global structural change.

Time-course analysis

When assuming only one conformation for the M-intermediate, the time course of the absorption change at 410 nm must be described by the V_2 component determined from the time-resolved diffraction data (Fig. 3 *d*). However, it is impossible to reconstitute the M-intermediate fraction in the absorbance by the time course from V_2 spectra. This fact confirms the presence of two substates in the M-intermediate. The L-intermediate also arises in BR photocycle at the time range we observed. Because only two structural states were identified in the diffraction data, the structural information of the L-intermediate is mostly included in a time-independent base component, which contains information on the original BR and M_1 intermediates state at present resolution. In fact, structure models of the L-intermediate demonstrate very small conformational changes, which probably contribute to the intensity changes in much higher resolution than 7 Å (Royant et al., 2000; Lanyi and Schobert, 2003; Kouyama et al., 2004).

In conclusion, two structure states observed in this diffraction data are the late M (M_2) intermediate state and

a base state. The base state that has almost the same structure with the original BR state includes L, M_1 intermediate and the original BR states. And, the second SVD component corresponds to the difference between M_2 and BR. Therefore, V_2 corresponds to the concentration of the M_2 intermediate.

CORRELATION BETWEEN HYDRATION AND THE STRUCTURAL CHANGES IN THE M-INTERMEDIATE

Through studying the influences of humidity on the photocycle of BR, Váró and Lanyi (1991b) suggested that the M_1–M_2 transition became slowly under relative humidity of $<$85%. Thus, under the condition, the amount of the M_1 state would be larger than that at higher humidity. In static x-ray and neutron diffraction experiments on PM film of D96N-BR, the global structural change of the M-intermediate observed under relative humidity higher than 75%, but the change was invisible at lower than 57% (Sass et al., 1997; Weik et al., 1998). Thus, the M1–M2 transition is expected to occur at ~75% relative humidity. Neutron inelastic scattering experiments on PM showed that anharmonic motion appeared above 250 K in BR incubated at 75% relative humidity or higher, but were silent at 57% and 0% (Lehnert et al., 1998). These observations suggest that the hydration level of BR molecules is profoundly important for anharmonic motions essential for inducing the M_1–M_2 transition. But static x-ray diffraction studies on purple membranes revealed that the deprotonation process of the Schiff base correlates with the global structural transition (Kataoka et al., 1994; Brown et al., 1997). If the deprotonation and the structural transition are coupled tightly, the global structural change would occur just after the deprotonation of the Schiff base. But this observation shows that the global structural change occurs ~5 ms after the deprotonation of the Schiff base. Anharmonic motions pointed out by the neutron experiment may appear in the M_1–M_2 transition and conduct the subsequent large conformational changes occurring in a delayed period from the deprotonation of the Schiff base.

We are grateful to Prof. M. Nasakasko for critical reading of the manuscript. The synchrotron radiation experiments were performed at the SPring-8 with the approval of the Program Review Committee of the Japan Synchrotron Radiation Research Institute (proposal No. 2002A0072-NL2-np, 2002B0263-NL2-np, and 2003A0172-NL2-np).

This research was partially supported by the Ministry of Education, Science, Sports and Culture, grants-in-aids 14780519 and 15076210 to T.O. The SPring-8 Joint Research Promotion Scheme of the Japan Science and Technology Corp. also partially supported this research.

REFERENCES

Brown, L. S., H. Kamikubo, L. Zimanyi, M. Kataoka, F. Tokunaga, P. Verdegem, J. Lugtenburg, and J. K. Lanyi. 1997. A local electrostatic change is the cause of the large-scale protein conformation shift in bacteriorhodopsin. *Proc. Natl. Acad. Sci. USA.* 94:5040–5044.

Druckmann, S., N. Friedman, J. K. Lanyi, R. Needleman, M. Ottolenghi, and M. Sheves. 1992. The back photoreaction of the M intermediate in the photocycle of bacteriorhodopsin: mechanism and evidence for two M species. *Photochem. Photobiol.* 56:1041–1047.

Facciotti, M. T., S. Rouhani, F. T. Burkard, F. M. Betancourt, K. H. Downing, R. B. Rose, G. McDermott, and R. M. Glaeser. 2001. Structure of an early intermediate in the M-state phase of the bacteriorhodopsin photocycle. *Biophys. J.* 81:3442–3455.

Fujisawa, T., Y. Inoko, and N. Yagi. 1999. The use of a Hamamatsu x-ray image intensifier with a cooled CCD as a solution x-ray scattering detector. *J. Synchrotron Rad.* 6:1106–1114.

Hara, T., T. Tanaka, T. Seike, T. Bizen, X. Marechal, T. Kohda, K. Inoue, T. Oka, T. Suzuki, N. Yagi, and H. Kitamura. 2001. In-vacuum x-ray helical undulator for high flux beamline. *Nucl. Instrum. Methods Phys. Res. A.* 467–468:165–168.

Haupts, U., J. Tittor, and D. Oesterhelt. 1999. Closing in on bacteriorhodopsin: progress in understanding the molecule. *Annu. Rev. Biophys. Biomol. Struct.* 28:367–399.

Henderson, R., J. Baldwin, T. A. Ceska, F. Zemlin, E. Beckmann, and K. H. Downing. 1990. Model for the structure of bacteriorhodopsin based on high-resolution electron cryo-microscopy. *J. Mol. Biol.* 213:899–929.

Henry, E. R., and J. Hofrichter. 1992. Singular value decomposition: application to analysis of experimental data. *Methods Enzymol.* 210:129–192.

Inoue, K., T. Oka, T. Suzuki, N. Yagi, K. Takeshita, S. Goto, and T. Ishikawa. 2001. Present status of high flux beamline (BL40XU) at SPring-8. *Nucl. Instrum. Methods Phys. Res. A.* 467/468:674–677.

Kamikubo, H., M. Kataoka, G. Váró, T. Oka, F. Tokunaga, R. Needleman, and J. K. Lanyi. 1996. Structure of the N intermediate of bacteriorhodopsin revealed by x-ray diffraction. *Proc. Natl. Acad. Sci. USA.* 93: 1386–1390.

Kamikubo, H., T. Oka, Y. Imamoto, F. Tokunaga, J. K. Lanyi, and M. Kataoka. 1997. The last phase of the reprotonation switch in bacteriorhodopsin: the transition between the M-type and the N-type protein conformation depends on hydration. *Biochemistry.* 36:12282–12287.

Kataoka, M., H. Kamikubo, F. Tokunaga, L. S. Brown, Y. Yamazaki, A. Maeda, M. Sheves, R. Needleman, and J. K. Lanyi. 1994. Energy coupling in an ion pump. The reprotonation switch of bacteriorhodopsin. *J. Mol. Biol.* 243:621–638.

Kouyama, T., T. Nishikawa, T. Tokuhisa, and H. Okumura. 2004. Crystal structure of the L intermediate of bacteriorhodopsin: evidence for vertical translocation of a water molecule during the proton pumping cycle. *J. Mol. Biol.* 335:531–546.

Lanyi, J., and B. Schobert. 2002. Crystallographic structure of the retinal and the protein after deprotonation of the Schiff base: the switch in the bacteriorhodopsin photocycle. *J. Mol. Biol.* 321:727–737.

Lanyi, J. K., and B. Schobert. 2003. Mechanism of proton transport in bacteriorhodopsin from crystallographic structures of the K, L, M1, M2, and M2' intermediates of the photocycle. *J. Mol. Biol.* 328:439–450.

Lanyi, J. K., and B. Schobert. 2004. Local-global conformational coupling in a heptahelical membrane protein: transport mechanism from crystal structures of the nine states in the bacteriorhodopsin photocycle. *Biochemistry.* 43:3–8.

Lehnert, U., V. Reat, M. Weik, G. Zaccai, and C. Pfister. 1998. Thermal motions in bacteriorhodopsin at different hydration levels studied by neutron scattering: correlation with kinetics and light-induced conformational changes. *Biophys. J.* 75:1945–1952.

Luecke, H., B. Schobert, J.-P. Cartiller, H.-T. Richter, A. Rosengarth, R. Needleman, and J. K. Lanyi. 2000. Coupling photoisomerization of retinal to directional transport in bacteriorhodopsin. *J. Mol. Biol.* 300:1237–1255.

Luecke, H., B. Schobert, H.-T. Richter, J.-P. Cartailler, and J. K. Lanyi. 1999. Structural changes in bacteriorhodopsin during ion transport at 2 angstrom resolution. *Science.* 286:255–260.

Nakasako, M., M. Kataoka, Y. Amemiya, and F. Tokunaga. 1991. Crystallographic characterization by x-ray diffraction of the M-intermediate from the photo-cycle of bacteriorhodopsin at room temperature. *FEBS Lett.* 292:73–75.

O'Brien, F. E. M. 1948. The control of humidity by saturated salt solutions. *J. Sci. Instruments.* 25:73–76.

Oesterhelt, D., and W. Stoeckenius. 1974. Isolation of the cell membrane of Halobacterium halobium and its fractionation into red and purple membrane. *Methods Enzymol.* 31:667–678.

Oka, T., K. Inoue, and N. Yagi. 2004. Microsecond time-resolved diffraction and scattering measurements system using semi-monochromatic x-ray pulse at SPring-8 BL40XU. AIP Conf. Proc. 705:1197–1200.

Oka, T., N. Yagi, T. Fujisawa, H. Kamikubo, F. Tokunaga, and M. Kataoka. 2000. Time-resolved x-ray diffraction reveals multiple conformations in the M-N transition of the bacteriorhodopsin photocycle. *Proc. Natl. Acad. Sci. USA.* 97:14278–14282.

Oka, T., N. Yagi, F. Tokunaga, and M. Kataoka. 2002. Time-resolved x-ray diffraction reveals movement of F helix of D96N bacteriorhodopsin during M-MN transition at neutral pH. *Biophys. J.* 82:2610–2616.

Rödig, C., and F. Siebert. 1999. Distortion of the L→M transition in the photocycle of the bacteriorhodopsin mutant D96N: a time-resolved step-scan FTIR investigation. *FEBS Lett.* 445:14–18.

Royant, A., K. Edman, T. Ursby, E. Pebay-Peyroula, E. M. Landau, and R. Neutze. 2000. Helix deformation is coupled to vectorial proton transport in the photocycle of bacteriorhodopsin. *Nature.* 406:645–648.

Sass, H. J., I. W. Schachowa, G. Rapp, M. H. Koch, D. Oesterhelt, N. A. Dencher, and G. Buldt. 1997. The tertiary structural changes in bacteriorhodopsin occur between M states: x-ray diffraction and Fourier transform infrared spectroscopy. *EMBO J.* 16:1484–1491.

Sass, H., J. G. Büldt, R. Gessenich, D. Hehn, D. Neff, R. Schlesineger, J. Berendzen, and P. Ormos. 2000. Structural alterations for proton translocation in the M state of wild-type bacteriorhodopsin. *Nature.* 406:649–653.

Váró, G., and J. K. Lanyi. 1991a. Kinetic and spectroscopic evidence for an irreversible step between deprotonation and reprotonation of the Schiff base in the bacteriorhodopsin photocycle. *Biochemistry.* 30:5008–5015.

Váró, G., and J. K. Lanyi. 1991b. Distortions in the photocycle of bacteriorhodopsin at moderate dehydration. *Biophys. J.* 59:313–322.

Váró, G., and J. K. Lanyi. 1991c. Thermodynamics and energy coupling in the bacteriorhodopsin photocycle. *Biochemistry.* 30:5016–5022.

Weik, M., G. Zaccai, N. A. Dencher, D. Oesterhelt, and T. Hauss. 1998. Structure and hydration of the M-state of the bacteriorhodopsin mutant D96N studied by neutron diffraction. *J. Mol. Biol.* 275:625–634.

Zimanyi, L., G. Váró, M. Chang, B. Ni, R. Needleman, and J. K. Lanyi. 1992. Pathways of proton release in the bacteriorhodopsin photocycle. *Biochemistry.* 31:8535–8543.